ASSESSMENT OF ABSORBED DOSE TO THE EYE'S LENS DURING DENTAL CBCT WITH DIFFERENT ACQUISITION PROTOCOLS

NUR AIMI FATIHAH BINTI MD ZUMZURI

SCHOOL OF HEALTH SCIENCES UNIVERSITI SAINS MALAYSIA

ASSESSMENT OF ABSORBED DOSE TO THE EYE'S LENS DURING DENTAL CBCT WITH DIFFERENT ACQUISITION PROTOCOLS

By

NUR AIMI FATIHAH BINTI MD ZUMZURI

Dissertation submitted in partial fulfilment of the requirement for the

Degree of Bachelor of Medical Radiation with Honours

JULY 2025

CERTIFICATE

This to certify that the dissertation entitled "ASSESSMENT OF ABSORBED DOSE

TO THE EYE'S LENS DURING DENTAL CBCT WITH DIFFERENT

ACQUISITION PROTOCOLS" is the bona fide record of research work done by NUR

AIMI FATIHAH BINTI MD ZUMZURI during the period from October 2024 to June

2025 under my supervision. I have read this dissertation and that in my opinion it

conforms to acceptable standards of scholarly presentation and is fully adequate, in scope

and quality, as a dissertation to be submitted in partial fulfilment for the degree of Degree

of Bachelor of Medical Radiation with Honours

Main Supervisor:

Co-Supervisor:

Associate Professor Dr. Diyana Binti Osman University Lecturer

Advanced Medical and Dental Institute

Universiti Sains Malaysia Bertam 13200 Kepala Batas Pulau Pinang, Malaysia

Puan Hanis Arina Binti Jaafar Radiographer Advanced Medical and Dental Institute Universiti Sains Malaysia Bertam 13200 Kepala Batas Pulau Pinang, Malaysia

......

Date: July 2025

iii

DECLARATION

I, Nur Aimi Fatihah Binti Md Zumzuri here declare that the dissertation entitled

"ASSESSMENT OF ABSORBED DOSE TO THE EYE'S LENS DURING DENTAL

CBCT WITH DIFFERENT ACQUISITION PROTOCOLS" is the result of my own

investigations, except where otherwise stated and duly acknowledged. I also declared that

it has not been previously or concurrently submitted as a whole for other degrees at

Universiti Sains Malaysia or other institutions. I grant Universiti Sains Malaysia the right

to use the dissertation for teaching, research and promotional purposes.

......

NUR AIMI FATIHAH BINTI MD ZUMZURI

Date: July 2025

iv

ACKNOWLEDGEMENT

In the name of Allah S.W.T., the Most Gracious and the Most Merciful. All praise to Him for His blessings and for giving me the opportunity to complete the research project my bachelor's degree. It is by His divine will, endless mercy, and boundless blessings that I have been granted the strength, patience, and opportunity to complete this final year project. It is crowning milestone of my bachelor's journey. This journey has not been easy. It was filled with sleepless nights, doubts, and many challenges. But along the way, there were also moments of joy, new experiences, and meaningful lessons that I will always remember. This phase of my life has taught me to be stronger and more mature.

Special thanks to my beloved mother, Muna Binti Ibrahim, and all my family members for their endless support emotionally, financially, and in every way needed throughout this project. My deepest gratitude also goes to my supervisor, Associate Professor Dr. Diyana Binti Osman. I am truly grateful to have such a kind, patient, and knowledgeable supervisor who was always willing to guide me and share her time to help me in completing this thesis. I would also like to express my sincere appreciation to my co-supervisor, Puan Hanis Arina Jaafar, and the staff of Imaging Unit, PPUSMB and PhD's student at AMDI for their invaluable assistance, especially during the data collection process. Their support made it all possible. I am deeply thankful to my significant other, Amir Zulhasmunizan, as well as my close friends, Andriana Othman, Akma Nazim, Amirah Atikah, and Azmin Aina for their unwavering love and constant support, whether emotional, financial, or mental, throughout this journey. Their presence was truly invaluable, especially during the most stressful moments and the ones I will always cherish. I could not have completed this study without them.

Lastly, I would like to thank all my classmates. I am forever grateful for their presence, kindness, and support throughout these four unforgettable years. I sincerely wish each of them happiness and success in all their future pursuits.

TABLE OF CONTENTS

CERTIFICATE	iii
DECLARATION	iv
ACKNOWLEDGEMENT	v
TABLE OF CONTENTS	vii
LIST OF FIGURES	ix
LIST OF TABLES	xi
LIST OF ABREVATION	xii
ABSTRAK	xiii
ABSTRACT	XV
CHAPTER 1: INTRODUCTION	1
1.1 Background of Study	1
1.2 Problem Statement	2
1.3 Research Objective	3
1.3.1 General Objective:	3
1.3.2 Specific Objectives:	3
1.4 Study Hypothesis	3
1.4.1 Null hypothesis:	3
1.4.2 Alternative hypothesis:	3
1.5 Research Question	4
1.6 Significance of Study	4
CHAPTER 2: LITERATURE REVIEW	5
2.1 CBCT in Dental Imaging	5
2.2 Radiosensitivity of the Eye Lens	7
2.3 Eye Lens Dose Limit	9
2.4 Effect of Radiation to Eye Lens	10
2.5 Measurement of the Dose to Eye Lens in Diagnostic Imaging.	12
2.6 Principles of Thermoluminescent Dosimeter (TLD)	16
2.7 Comparison Dose-Area-Product (DAP) and Computed Tomographic Do	se Index
(CTDI) in dental CBCT.	21
CHAPTER 3: RESEARCH METHODOLOGY	22
3.1 Study Design	22
3.2 Study Location	23
3 3 Research Tools	23

3.3.1 ATOM Max Dental and Diagnostic Head Phantom Model 711-HN	23
3.3.2 Planmeca ProMax® 3D Mid Cone Beam Computed Tomography.	25
3.3.3 SIEMENS Digital Radiography (DR) Systems.	27
3.3.4 Thermoluminescence Dosimeter 100 (TLD-100)	28
3.3.5 Unfors RaySafe Xi R/F Dosimeter	29
3.4 Research Methodology	30
3.4.1 TLD Sensitivity Test	30
3.4.2 TLD Calibration	32
3.4.3 Eye Lens Dose Measurement with Head Phantom Study	37
CHAPTER 4: RESULTS AND DISCUSSION	40
4.1 Sensitivity Test of TLD Chips	40
4.2 Calibration curve of TLD-100 Chip	42
4.3 Measurement of Absorbed Dose to Eye Lens on Head Phantom	43
4.4 CTDI _{vol} and DAP as references in Absorbed Dose Measurement of Head Phantom	50
4.5 Limitation of Study	55
CHAPTER 5: CONCLUSION	58
5.1 Conclusion	58
5.2 Future recommendations	58
REFERENCES	61
APPENDICES	64
APPENDIX 1	64
APPENDIX 2	65
APPENDIX 3	66
APPENDIX 4	67

LIST OF FIGURES

Figure 2.1 The basic CBCT scan principles includes rotation of the gantry with an x-ray tube and image detector (T. Kaasalainen et al., 2021)
,
Figure 2.2 Schematic diagram the radiosensitive region of the eye lens (Bandaran et.al,
2019) 7
Figure 2.4 shows the position of the lead patch on the SK-150 head phantom (Xiong et
al., 2020)
Figure 2.5 Positions of TLDs attached on the top border of respiratory/surgical mask
below the eye region (Hatama et al. 2020)
Figure 2.6 (a) Simplified energy level diagram representing the delocalized bands
(valence band and conduction band) and the electronic transitions in Thermoluminescent
luminescent material during irradiation (a) and readout (b) where stimulation is provided
by heat o or light (Stephen et. al, 2020)
Figure 2.6 (b) shows the Thermoluminescent curves of LiF:Mg,Ti (TLD-100) subjected
to different pre-irradiation annealing treatments 18
Figure 2.6 (c) shows basic elements of (a) a thermoluminescent dosimeters reader 19
Figure 3.2 This study was conducted at Institut Perubatan dan Pergigian Termaju
Advanced Medical and Dental Institute (IPPT) 23
Figure 3.3.1 ATOM Max Dental and Diagnostic Head Phantom Model 711-HN (PEO
Medical, 2015) 24
Figure 3.3.2 Planmeca ProMax® 3D Mid Cone Beam Computed Tomography (CBCT)
(Equipment, H.S. 2021) 25
Figure 3.3.3 Siemens YSIO X.pree Digital Radiography (DR) general x-ray system
(Siemens Healthnieers, n.d) 27
Figure 3.3.4 The TLDs-100 chips placed on the chips holder 28
Figure 3.3.5 shows the briefcase of Unfors Raysafe Xi R/F Dosimeter
Figure 3.4 The flowchart of performing TLD-100 chips for sensitivity, calibration curve,
and CBCT scanning with different acquisition protocols test.
Figure 3.4.1 shows the TLD chips on the beam collimator 10 cm x 10cm
Figure 3.4.2(a) shows 50 TLD-100 chips were arranged and sorted in the annealing
planchet with acrylic cover plate according to their label. 32 33 34 30 31 32 33 33 34 36 36 37 38 38 39 30 30 30 30 30 30 30 30 30
Figure 3.4.2(b) shows TLD furnace Type LAB-01/400 annealing oven was used.
Figure 3.4.2(c) shows Three TLD chips were used for each exposure and were placed
beside the RaySafe Unfors dosimeter within same field of view (FOV) and beam
collimator 10 cm x 10cm. 34
Figure 3.4.2 (d) shows Harshaw 3500 TLD Reader.
Figure 3.4.2(e) shows the drawer position is 'between'
Figure 3.4.2(f) shows the position of drawer is opened.
Figure 3.4.3(a) shows Two TLD-100 chips were placed on the eye lens right and left of
head phantom surface. 37
Figure 3.4.3(b) shows the TLD chip was placed on the eye lens surface by using white
tape 38

Figure 3.4.3(c) shows the set-up head phantom with stand and CBCT Figure 4.1 The sensitivity graph of TLD-100 Figure 4.2 The graph of calibration curve for TLD-100 Chips.	39 41 42		
		Figure 4.3 Graph of absorbed dose to lens at different exposure setting, kVp	44

LIST OF TABLES

43
p
46
1
48
ed
50
ed
52
L
53
64
65
66
67

LIST OF ABREVATION

AMDI Advanced Medical and Dental Institute

IPPT Institut Perubatan dan Pergigian Termaju

USM Universiti Sains Malaysia

CBCT Cone Beam Computed Tomography

CT Computed Tomography

CTDI Computed Tomography Dose Index

DAP Dose-Area Product

DR Digital Radiography

FOV Field of View

HVL Half-Value Layer

kVp kiloVoltage Peak

mA milliAmpere

mAs Milliampere-seconds

QA Quality Assurance

TLD Thermoluminescent Dosimeter

TLD-100 Thermoluminescent Dosimeter (LiF:Mg,Ti) type 100

μGy MicroGray

μm Micrometer

PENILAIAN DOS TERSERAP PADA KANTA MATA SEMASA CBCT PERGIGIAN DENGAN PROTOCOL PEMEROLEHAN YANG BERBEZA

ABSTRAK

Tomografi berkomputer sinar-X berkon beam (CBCT) kini diiktiraf sebagai satu kaedah pencitraan penting dalam bidang pergigian moden kerana kemampuannya menghasilkan imej tiga dimensi (3D) beresolusi tinggi dengan dos sinaran yang lebih rendah berbanding CT konvensional. Walau bagaimanapun, CBCT masih mendedahkan organ sensitif seperti kanta mata kepada risiko sinaran, yang berpotensi meningkatkan kebarangkalian pembentukan katarak akibat radiasi. Kajian ini dijalankan bagi menilai dos terserap pada kanta mata semasa prosedur CBCT pergigian dengan menggunakan dosimeter termoluminesen TLD-100 (TLD), serta menganalisis kesan perubahan parameter pendedahan terhadap tahap dos yang diterima. Satu fantom kepala antropomorfik 3D digunakan bagi mensimulasikan seorang pesakit, dan cip TLD diletakkan dengan teliti pada kedudukan anatomi kanta mata kanan dan kiri. Fantom tersebut didedahkan kepada pelbagai protokol pengimbasan CBCT dengan variasi dalam saiz medan pandangan (FOV), voltan tiub (kVp), dan arus tiub (mA). Keputusan menunjukkan bahawa dos terserap kepada kanta mata dipengaruhi oleh perubahan FOV dan mA. Pada FOV tetap (saiz M) dan 8 mA, peningkatan kVp dari 60 ke 90 menyebabkan peningkatan dos daripada 0.778 mGy kepada 1.563 mGy. Apabila mA ditingkatkan daripada 3.2 kepada 16 pada 60 kVp, dos yang diperoleh berada dalam julat 0.420 mGy hingga 4.412 mGy. Selain itu, pada kVp tetap 90, peningkatan FOV daripada XS ke XL menunjukkan dos purata kanta mata antara 2.148 mGy hingga 3.093 mGy. Kajian ini menyeru kepada pengoptimuman protokol pengimbasan serta penggunaan faktor pembetulan tenaga dalam mengurangkan pendedahan sinaran yang tidak perlu. Langkah pengurangan dos

dan kesedaran dalam kalangan pengamal pergigian adalah penting dalam memastikan kesejahteraan pesakit, khususnya bagi prosedur yang melibatkan pengimbasan berulang.

Kata kunci: CBCT pergigian, dos kanta mata, TLD-100, dosimetri radiasi

ASSESMENT OF ABSORBED DOSE TO THE EYE'S LENS DURING DENTAL CBCT WITH DIFFERENT ACQUISITION PROTOCOLS

ABSTRACT

Dental cone-beam computed tomography (CBCT) is widely recognised as a valuable imaging modality in modern dentistry, offering high-resolution, three-dimensional images with relatively lower radiation exposure compared to conventional CT. Despite its advantages, CBCT still poses radiation risks to radiosensitive organs, particularly the eye lens, which has been linked to an increased risk of radiation-induced cataracts. This study was conducted to evaluate the absorbed dose to the eye lens during dental CBCT procedures using TLD-100 thermoluminescent dosimeters (TLDs), and to examine how variations in scanning parameters influence dose levels. A 3D anthropomorphic head phantom was employed to replicate a human, with TLDs was positioned at the specific locations of both eye lenses. The phantom was scanned using different CBCT exposure protocols, varying in field of view (FOV), tube voltage (kVp), and tube current (mA). The results demonstrated that absorbed dose to the eye lens was influenced by both FOV and mA settings. At a fixed FOV (medium size) and 8 mA, an increase in kVp from 60 to 90 resulted in increased eye lens dose from 0.778 mGy to 1.563 mGy. Conversely, when mA was varied from 3.2 to 16 mA at 60 kVp, the dose ranged from 0.420 mGy to 4.412 mGy. Additionally, under a constant 90 kVp setting, increasing FOV from XS to XL produced mean eye lens doses ranging from 2.148 mGy to 3.093 mGy. The use of TLD-100 dosimeters proved reliable in dose measurement, reinforcing the importance of accurate dosimetry for patient protection. This study underscores the need for optimised scanning protocols and consideration of energy correction factors to reduce unnecessary radiation exposure. Implementing dose-reduction strategies and increasing awareness

among dental professionals can ensuring patients safety, particularly in procedures requiring repeated imaging.

Keywords: Dental CBCT, eye lens dose, TLD-100, radiation dosimetry

CHAPTER 1

INTRODUCTION

1.1 Background of Study

Cone-beam computed tomography (CBCT) is a modern imaging technique that has gained popularity in dental diagnostic due to its ability to provide high-resolution, three-dimensional (3D) images. It is commonly used for evaluating impacted teeth and assessing mandibular prior to implant placement (Kanzaki et al., 2017). While it offers significant benefits in clinical diagnosis and treatment planning, its increasing use also raises concerns on radiation exposure, particularly to sensitive tissue such as the eye lens. The eye lens is recognised as a radiosensitive organ, and exposure to ionising radiation can lead to detrimental effects, including cataracts, especially when cumulative doses exceed 100 mGy (Pauwels, et al., 2014). The growing concern regarding radiation exposure to the eye lens during dental CBCT procedures centres on the absorbed dose received by this sensitive organ. Several factors influence the absorbed dose to the eye lens, including the field of view (FOV), tube current, and exposure time. Understanding the correlation between these parameters and the absorbed dose to the eye lens is essential in optimising imaging protocols, aiming to minimise exposure while maintaining diagnostic efficacy.

1.2 Problem Statement

With the increasing use of dental CBCT, there is a growing concern about the potential rise in radiation exposure, particularly to radiosensitive tissue such as the eye lens. Although the primary focus of CBCT imaging is on dental structures, the positioning and proximity of the x-ray beam can result in unintended exposure to the eye lens. This is particularly critical as the eye lens is highly susceptible to radiation-induced damage, which can lead to serious health effects such as cataracts (ICRP, 2011). The risk is further amplified in paediatric patients, whose developing tissues are more sensitive to radiation. This requires a thorough investigation of the absorbed dose to the lens of the eye during various acquisition protocols.

However, there is a lack of comprehensive evaluation of the factors influencing the absorbed dose to the eye lens during dental CBCT procedures. Additionally, the correlation between these factors such as absorbed dose, the size of the irradiated area, dose metric like dose area product (DAP) and computed tomography dose index (CTDI) remains underexplored. Furthermore, findings from this research could assist in developing standardised CBCT imaging protocols that effectively mitigate the risks associated with radiation exposure to the eye lens, thereby enhancing patient safety without compromising diagnostic quality.

1.3 Research Objective

1.3.1 General Objective:

This study aims to determine the absorbed dose to the eye's lens during dental CBCT using difference acquisition protocols, measured with thermoluminescent dosimeters (TLDs).

1.3.2 Specific Objectives:

- To measure the absorbed dose to eye lens using TLDs in a phantom study.
- To examine the correlation between different CBCT protocols and the absorbed doses to the eye's lens.
- To examine the correlation between displayed dose, dose-area product (DAP) and CTDI with the measured absorbed dose to eyes lens.

1.4 Study Hypothesis

1.4.1 Null hypothesis:

- There is no significance difference of the absorbed dose to the eye lens between different CBCT protocols.
- There is no significance correlation between the associated factors with the measured absorbed doses to the eye lens

1.4.2 Alternative hypothesis:

- There is a significant difference of the absorbed dose to the eye lens between different CBCT protocols.
- There is significant correlation between the associated factors with the measured absorbed doses to the eye lens.

1.5 Research Question

This study is guided by the following research questions:

- What is the absorbed dose to the eye lens during dental CBCT procedures using different acquisition protocols?
- How do variations in CBCT parameters such as field of view (FOV), tube current, and exposure time affect the absorbed dose to the eye lens?
- How is the correlation between dose-area product (DAP) and CTDI with the absorbed dose to the eye lens in dental CBCT scans?

1.6 Significance of Study

This study aims to enhance patient safety by investigating the absorbed dose to the eye lens during dental CBCT scans, an area of concern due to the lens's high sensitivity to ionising radiation. Besides that, it examines how different acquisition protocols influence radiation dose by exploring the correlation between key dose metrics, such as dose-area-product (DAP) and computed tomography dose index (CTDI), and the absorbed dose to the eye lens. The findings will contribute to the optimisation of CBCT acquisition protocols, enabling reduced radiation exposure without compromising image quality. Furthermore, this finding will help to promote patient safety of eye lenses from cataract formation. Meanwhile, this study supports the development of evidence-based guidelines and recommendations to improve radiological safety in dental imaging, in line with the ALARA (As Low as Reasonably Achievable) principle.

CHAPTER 2

LITERATURE REVIEW

This chapter presents a review of existing literature related to radiation exposure from dental CBCT procedures, with particular emphasis on the sensitivity of the eye lens to ionising radiation. It explores key aspects such as established dose limits, the biological impact of radiation on the eye lens, and techniques commonly used for dose assessment, especially the use of thermoluminescent dosimeters (TLD-100). Furthermore, dose measurement indices, including Dose-Area Product (DAP) and Computed Tomography Dose Index (CTDI), are examined to support the evaluation of absorbed dose in CBCT imaging.

2.1 CBCT in Dental Imaging

Cone-beam computed tomography (CBCT) overcomes the limitations of traditional two-dimensional dental imaging and enables accurate depiction of multiplanar details of maxillofacial bony structures and surrounding soft tissues (Kaasalainen et. al., 2021). As shown in Figure 1, the principle of cone beam computed tomography (CBCT) works by using an X-ray tube and a detector that rotate around the patient. As the tube

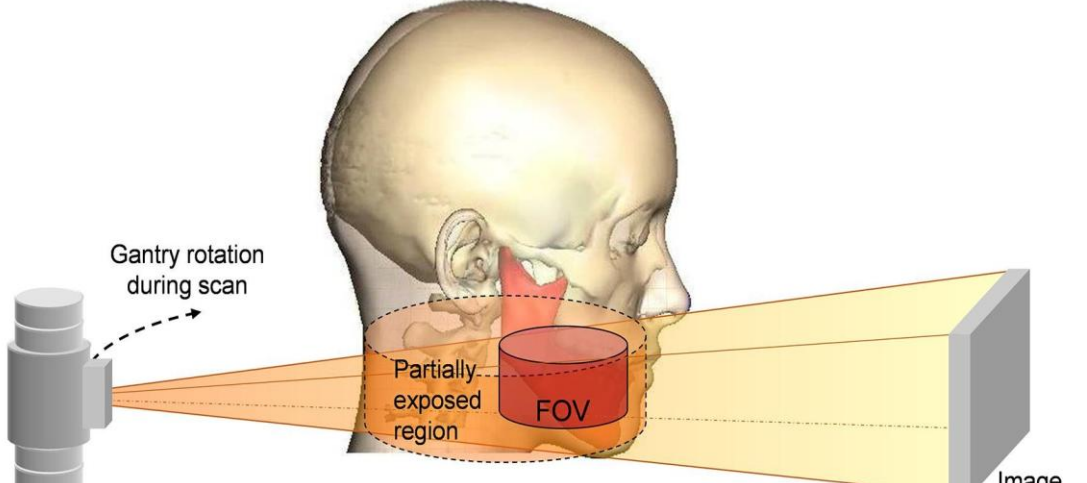


Figure 2.1 The basic CBCT scan principles includes rotation of the gantry with an x-ray tube and image detector (T. Kaasalainen et al., 2021)

emits X-rays from one side, the detector on the opposite side records how much of the X-rays pass through the body. This creates detailed 3D images of the scanned area.

CBCT systems use continuous or pulsed exposure. In dental CBCT, pulsed exposure is more common because it shortens the exposure time and helps reduce the radiation dose to the patient. The way X-rays interact with the body depends on the materials they pass through. Two main interactions occur: the photoelectric effect and Compton scattering. The photoelectric effect is mainly responsible for image contrast, especially at lower energy levels. However, as the tube voltage increases, this effect decreases, and image contrast is reduced. Meanwhile, scattered radiation increases with higher energy X-rays, which can reduce image quality (T. Kaasalainen et al., 2021)

In addition, Xiang et. al (2024) reported that the technological advanced which is including AI-assisted CBCT segmentation and low-dose radiation reconstruction. These technologies are enhancing diagnostics capabilities while aiming to reduce radiation exposure. Xiang et. al (2024) demonstrated that machine-learning algorithms have improved both the accuracy and speed of tooth segmentation from CBCT, while Giroux et. al (2024) showed that iterative reconstruction can maintain image quality under reduced-dose protocols.

2.2 Radiosensitivity of the Eye Lens

Cone-Beam Computed Tomography (CBCT) is widely used in dental imaging to provide high-resolution, three-dimensional (3D) images with low dose radiation. However, radiation exposure to the eye lens remains a significant concern due to its high radiosensitivity. The eye lens is one of the most radiosensitive tissues in the human body, and even relatively low doses of ionising radiation can induce damage. The most sensitive regions of the eye lens are estimated to be at a depth of 2–4 mm (shown as red regions), as illustrated in Figure 2 (Bandaran et. al, 2019)

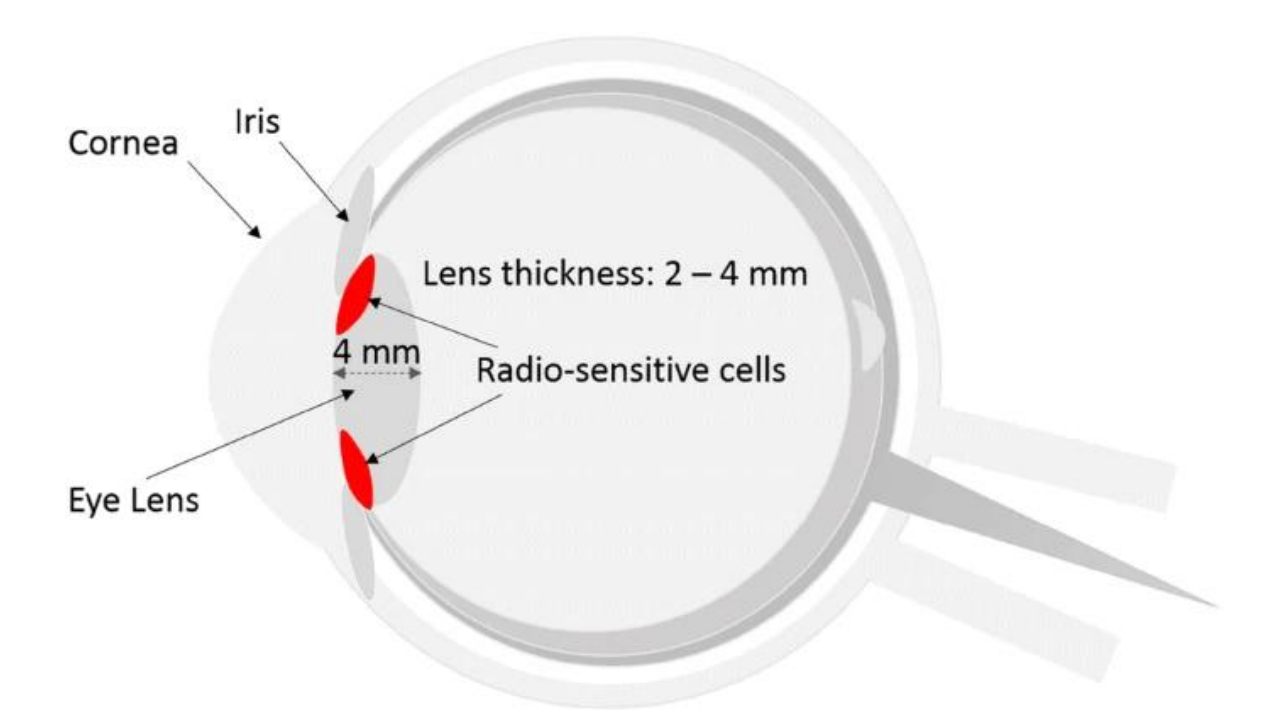


Figure 2.2 Schematic diagram the radiosensitive region of the eye lens (Bandaran et.al, 2019)

Recent studies and ICRP recommendations have indicated that the threshold dose for radiation-induced cataract formation is lower than previously reported, making the eye lens particularly susceptible to radiation-induced cataract genesis, with detectable effects observed at doses as low as 0.5 Gy (Ainsbury et al., 2021; ICRP 2011). This has prompted extensive investigations into dose optimisation strategies to protect the lens, particularly in procedures involving fluoroscopy or CT, where the eyes may be within or

near the primary radiation field. Assessment of the absorbed dose is essential for establishing safety guidelines and optimising imaging protocols authentically.

Several studies have investigated the impact of various CBCT acquisition protocols on the dose delivered to the eye lens. These various acquisition parameters in dental CBCT protocols include field of view (FOV) size, tube current (mA), tube voltage (kVp), rotation angle, voxel resolution, and scan time. Kanzaki et al. (2017) reported that the key factor influencing dose is the Field of View (FOV), and the absorbed doses to the eye lens reported during dental CBCT procedures typically range between 0.07 and 0.012 mGy. This is depending on the type of examination and imaging parameter performed.

2.3 Eye Lens Dose Limit

The potential for radiation-induced cataracts has made the eye lens a significant focus in radiation protection diagnostic imaging. The International Commission on Radiological Protection has accentuated the radiosensitivity of the eye lens by lowering the annual dose threshold. According to ICRP Publication 118, the recommended equivalent dose limit to the lens of the eye is 20 mSv per year, averaged over 5 years, with no single year exceeding 50 mSv (Principi et al., 2015). This modification reflects growing evidence that cataract formation occurs at lower radiation levels than previously assumed, reinforcing the need for strict occupational and patient exposure controls, particularly in high-risk areas like cone-beam computed tomography (CBCT) and interventional radiology.

Regarding scattered radiation to the eye lens, Khafaji and Albadawi (2023) reported a wide variation in doses during dental CBCT, ranging from 0.103 mSv to 8.3 mSv, and it depends on the scanner model, protocol settings, patient positioning, and protective measures. Furthermore, Alwasiah et al. (2021) found that in routine non-enhanced CT scans, the mean absorbed dose to the eye lens was 33.62 mGy. A level approaching thresholds associated with early lens opacities. Although this study focused on conventional CT, it highlights how even low-dose diagnostic procedures can contribute to significant cumulative radiation exposure when repeated or not properly optimized.

2.4 Effect of Radiation to Eye Lens

The formation of cataract is a form of lens opacity that can impair the vision of human. Radiation induced cataracts were considered as a deterministic effect within a relatively high threshold dose. Radiation-induced cataracts result from damage to the lens epithelial cells, which are responsible for maintaining the transparency and function of the lens.

Ionising radiation can induce DNA damage, apoptosis, or abnormal cell proliferation, leading to the accumulation of opacities over time (Hammer et al., 2013). Kleiman et al. (2012) found a significant increase in posterior subcapsular cataracts, even in individuals whose cumulative eye lens doses were below the earlier 150 mSv limit. It is also involved expose to interventional cardiologist and personnel.

For radiation protection, according to Xiong et al. (2020) the use of lateral lead shielding during CBCT could reduce the eye lens dose by up to 53%, as shown in Figure 2.4. In clinical environments, particularly for staff, personal dosimeters worn at eye level, and regular monitoring are essential for compliance with the ICRP's revised dose limits.

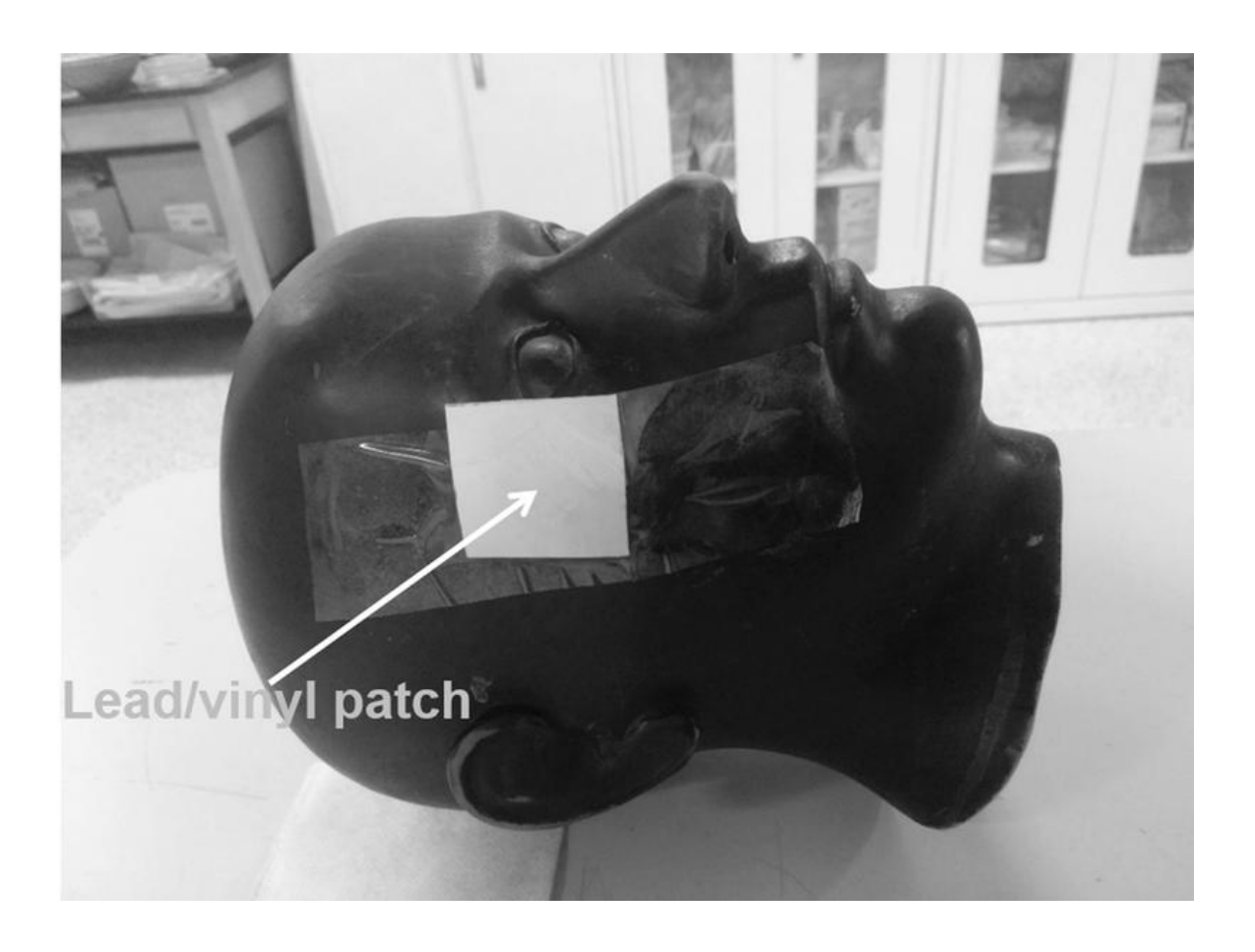


Figure 2.4 shows the position of the lead patch on the SK-150 head phantom (Xiong et al., 2020)

2.5 Measurement of the Dose to Eye Lens in Diagnostic Imaging.

Accurate quantification of the absorbed dose to the eye lens is significant due to lens's upsurged susceptibility to radiation-induced cataracts. There is an established approach to involve the use of TLDs. Thermoluminescent dosimeter (TLD) is one of the most effective and reliable tools for assessment, which is provides quantitative and reproducible radiation dose measurement. TLD-100, TLD-100H and TLD-700 series have been widely used due to their sensitivity, small size and tissue equivalent.

The study is about TLD-100 (LiF: Mg, Ti) and TLD-700H (LiF: Mg, Ti with reduced thermal fading)- combined with phantom studies. These TLDs, has stimulated as near tissue equivalence, sensitivity in low-dose ranges, and stability of dosimetric properties across photon energies typical of diagnostic imaging. TLDs is calibrated properly and effectively proven in evaluating lens doses from CBCT, interventional procedures and other radiographic modalities.

Pauwels et al. (2014) have evaluated the effective dose and dose to the eye lens dose from various dental CBCT modalities by using embedded TLDs in an anthropomorphic head phantom. It is one of the most detailed investigations. This detailed investigation used 148 TLDs placed at various head and neck locations, including the eye lens, to assess dose distribution.

Manna et. al (2023) has performed in-depth assessment of TLD-100's in interventional radiology to reflect the eye lens equivalent dose during lives procedures. This study for comparing and responding to the International Commission on Radiation Unit's recommended Hp (3) dosimeter. Their preliminary findings confirmed a strong correlation between the TLD-100 readings and the Hp (3) references values, indicating that the system is accurately calibrated for both energy response and angular dependence. TLD-100 is a reliable tool for eye lens dosimetry.

For radiation dose assessment, the anthropomorphic head phantom model is the main character which is accurately replicating human anatomy. A 3D-printed anthropomorphic head phantom is introduced by Endarko et al. (2023). It is fashioned from PLA and filled with stimulated brain and cerebrospinal fluid. After that, it is compared against a commercial CIRS standard phantom using a Cs-137 source. The effect of the angle of radiation source towards TLD reading at the anthropomorphic head phantom has a similar value to the standard phantom with a calibration factor ranging from 0.82 to 1. The absorbed dose measurement and the linear attenuation coefficient of the anthropomorphic head phantom with the standard phantom have different values of 2.52 and 3.78%, respectively. (Endarko et al. 2023).

For TLD positioning, the placement of TLDs at the phantom is significantly influences the dose values which is a critical consideration when examining eye-lens exposure. Inayah et al (2022) found that minor deviations in TLDs placement may lead to dose discrepancies of up to 18% and angular responses is also assessed for this finding. In addition, Filho et al. (2023) verified that persistence positioning within the eye socket or surrounding tissue is fundamental for reproducible dose measurement.

In reality of clinical environment, interventional radiologist and cardiologist worn Hp (3) badge dosimeter at eye level for recording the eye lens (Manna et al,2023) and a study of staff in Finland found that annual eye lens dose equivalent frequently approached or exceeded the new recommended limit of 20mSv/years. (Tapiovaara et al. 2020).

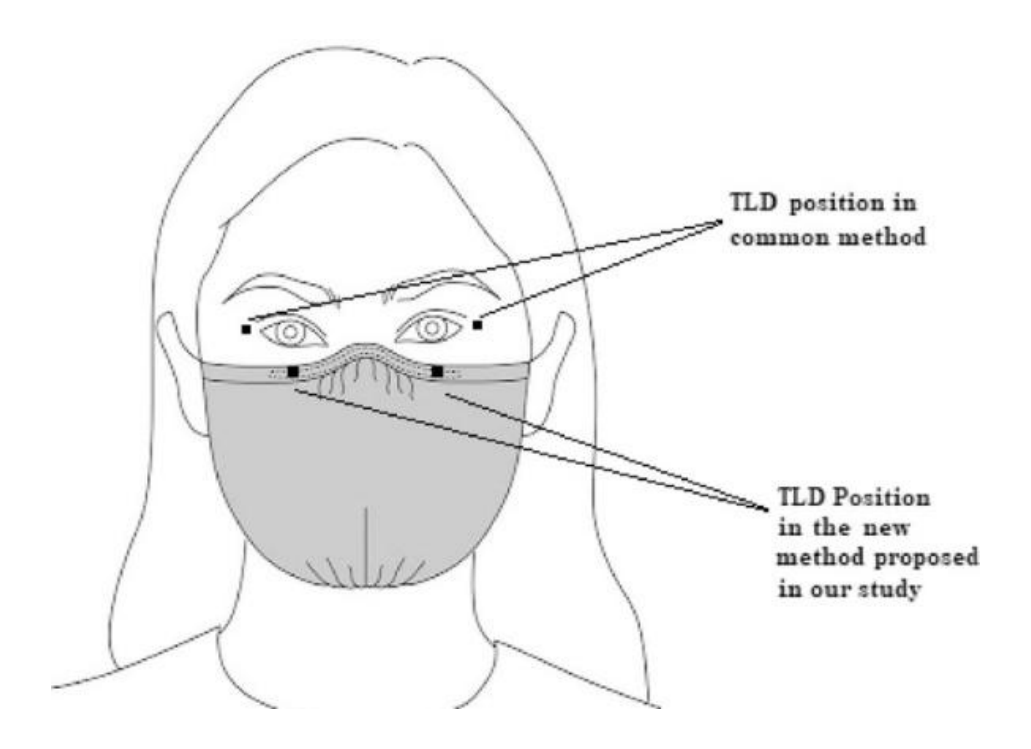


Figure 2.5 Positions of TLDs attached on the top border of respiratory/surgical mask below the eye region (Hatama et al. 2020)

Meanwhile, the Iranians studied and introduced a simplified TLD attachment method using surgical mask borders, and over 120 medical personnel were involved. In their common method, four TLDs are positioned near the left and right outer side using TLD holder as shown in Figure 2.5. It is fixed within taping the TLDs around their head. However, the placement of TLD method has been changed and placed at the upper border of the surgical mask below the eye area as new protocol for eye lens dose measurement (Hatami et al. 2020). In this clinical dosimetry is highlighted the benefits and limitations of both badge and eye-level monitoring.

Previous study by Pauwels et al., (2014) examined the effect of different tube rotation between full (360°) and half (180°) rotational protocols on the eye lens dose. The findings of this study reported that half-rotation protocols reduced the dose to the eye lens by up to 45% compared to full-rotation scans. Besides, they also reported that the eye lens dose varied widely, ranged between 95 μ Gy up to 6,861 μ Gy within depending on the

dental system and selected scan parameters. The highlight of this study is geometric factors such as gantry rotation angle can significantly influence dose distribution.

Moreover, the correlation between acquisition protocols and organ-specific doses has been furthered by Sharma et al.'s (2016) studies that evaluated eye lens doses using Optically Stimulated Luminescence (OSL) on a Varian On-Board Imaging (OBI) system used for image-guided radiotherapy (IGRT). In spite of OSLs being used, the dosimetry methodology is equivalent to the TLD-based approach within proper calibration. In this study, three CBCT acquisitions are compared, which are standard-dose head (SDH), high-quality head (HQH), and low-dose head (LDH). It is also found measurable differences in eye lens doses. These findings have confirmed that protocol choice, including image quality settings, can lead to two- to threefold changes in organ dose.

Moreover, Khafaji et al. (2023) used TLDs and OSLs in dental CBCT for conducting a systematic review compiling in eye lens doses. This study highlighted a wide variation in eye lens dose from as 0.1 mSv to over 8.3 mSv. It is primarily influenced by FOV size, patient positioning and scan settings. The analysis emphasized that the known sensitivity of the eye lens and the growing use of CBCT in routine practice, which is no universally adopted standard for eye lens dosimetry in dental imaging.

2.6 Principles of Thermoluminescent Dosimeter (TLD)

Thermoluminescent dosimeter such as TLD-100 (LiF: Mg, Ti) are widely used for measuring low-level radiation exposures due to their high sensitivity, dose linearity and tissue equivalence. AAPM Task Group 191 (2020), outlined essential handling and quality control protocols to ensure measurement accuracy within 1-2%. These include the use of non-contaminating tweezers, consistent annealing procedures, and reader stabilization.

A study by Borhani et al., (2021) assessed the thermoluminescent properties of TLD-100 alongside TLD--700H and GR200 within the 0.5–4.0 mGy- range, relevant to diagnostic imaging. While TLD-100 demonstrated good repeatability in accordance with IEC standards, it also showed more than 5% variability dependent on energy and doserate, an important consideration when measuring CBCT beams with varying spectra. The findings establish- that with rigorous calibration and procedural controls, TLD-100 remains appropriate for- eye-lens dosimetry in CBCT studies but remind researchers to account for its sensitivity to beam characteristics. (Borhani et al. 2021).

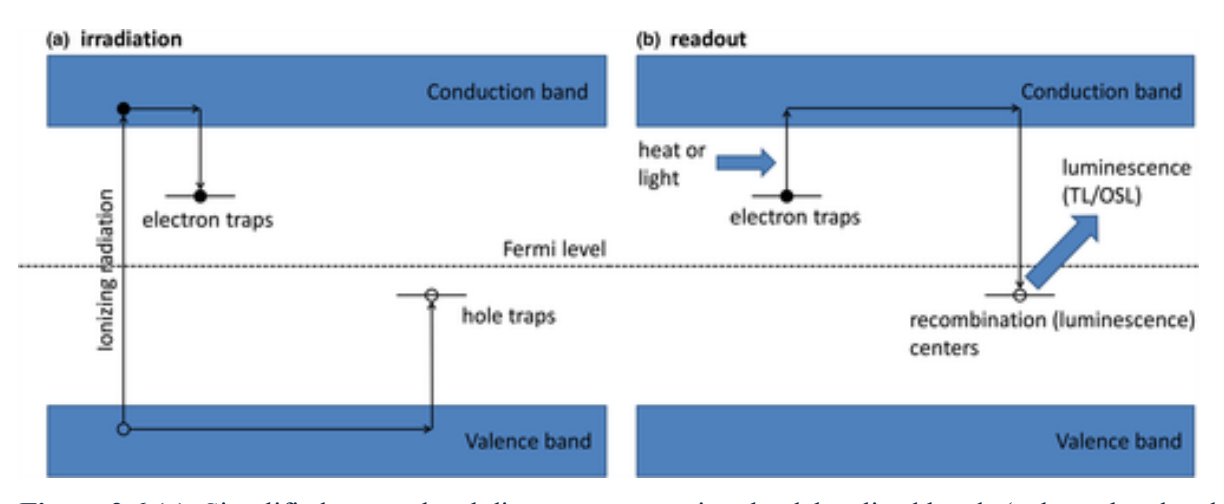


Figure 2.6 (a) Simplified energy level diagram representing the delocalized bands (valence band and conduction band) and the electronic transitions in Thermoluminescent luminescent material during irradiation (a) and readout (b) where stimulation is provided by heat o or light (Stephen et. al, 2020)

In a perfect crystalline insulator, the conduction and valence bands are separated by an energy difference of several eV, and there are no intermediate energy levels within this band gap. Luminescence detectors are created by adding impurities to these crystals, thereby introducing energy levels within the band gap in the vicinity of the impurities. As shown in Figure 2.6 (a), during exposure to ionising radiation ionizations created within the detector material promote a number of electrons to the conduction band, leaving behind holes in the valence band. These electrons and holes can move in their respective energy bands until they recombine or are captured by defects indicated by electron trap and hole trap. In the absence of additional stimuli such as heating or illumination, these trapped charges can remain trapped for periods ranging from less than one second to thousands of years, depending primarily on the trap depth, that is, the energy difference between the trap level and the delocalised conduction or valence band (Kry et al., 2020).

For reading process, stimulation by heat is releases the trapped charged. Once the trapped electron is released, it recombine with the trapped hole and a defect in the excited state is created. TLD result from the relaxation of the defect to return to the ground state by light emission. TLD reader stimulates the detector using heat and monitor the resultant luminescence with photomultiplier tube (PMT), which it convert the luminescence into counts.

To reading the TLD, the temperature of the detector is increasing while monitoring the TLD emitted, and a glow curve graph of signal vs temperature is created as shown in Figure 3. In the former, the TL signal can be defined as the maximum intensity of a TL peak or the integrated TL intensity over a region of interest (Kry et al., 2020).

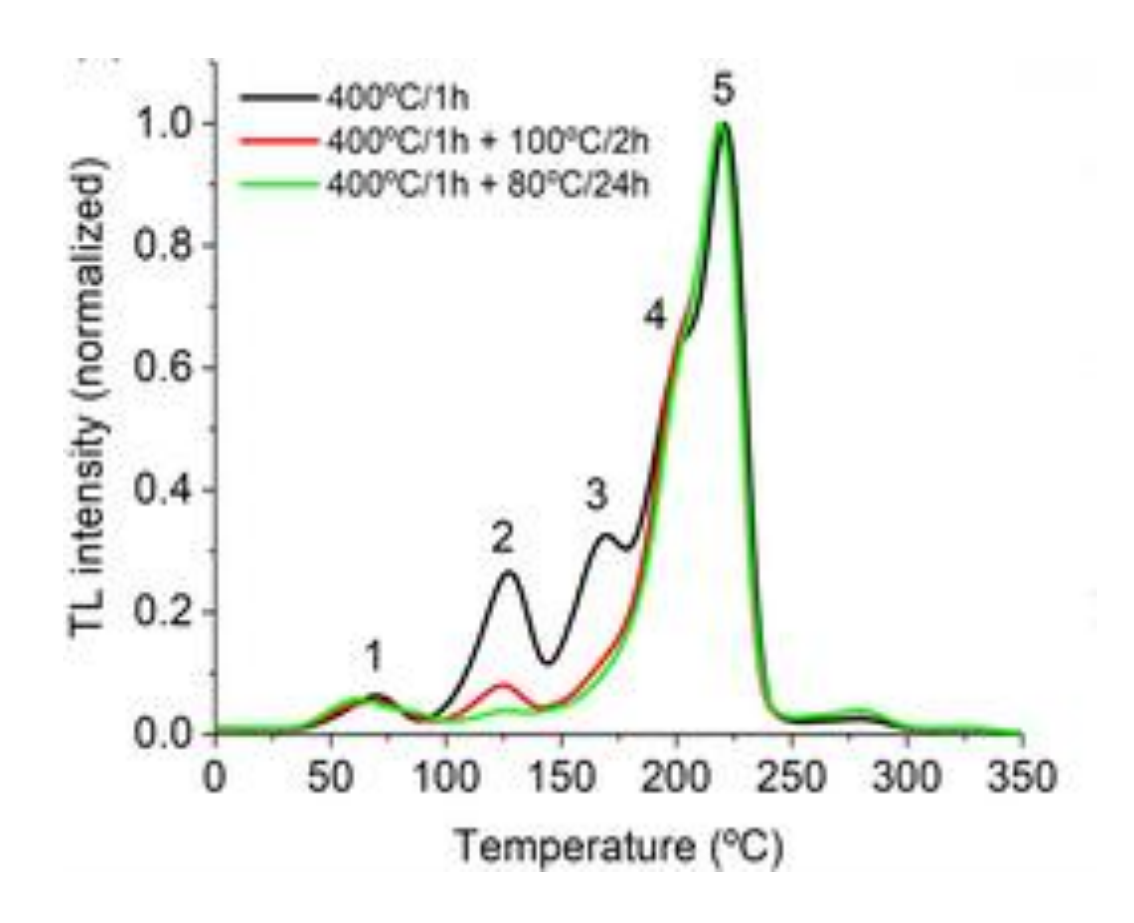


Figure 2.6 (b) shows the Thermoluminescent curves of LiF:Mg,Ti (TLD-100) subjected to different pre-irradiation annealing treatments

Stephen et. al (2020) stated and shown in Figure 2.6 (b) that different peaks can include different information about the irradiation, in clinical practice the standard practice is to simply integrate the entire glow curve to yield the overall signal. To ensure reproducible results, a consistent heating cycle should be used.

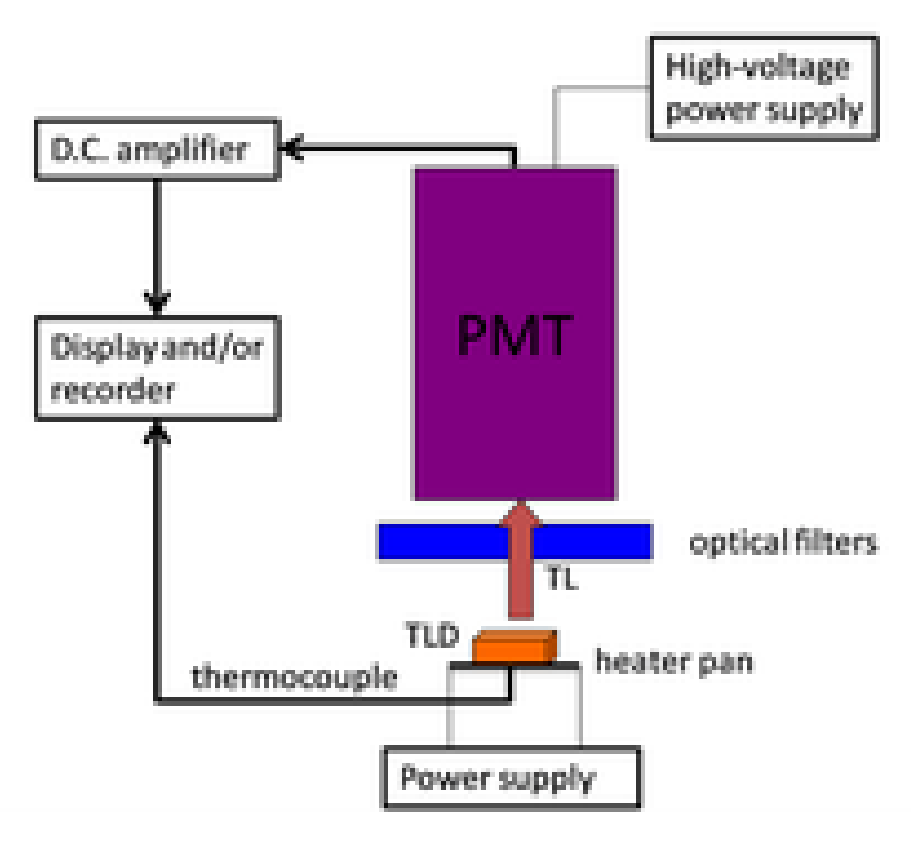


Figure 2.6 (c) shows basic elements of (a) a thermoluminescent dosimeters reader

Kry et. al (2020) reported that the calibration coefficients for identical irradiation conditions by the Imaging and Radiation Oncology Core (IROC) in Houston are shown for a TLD reader (Harshaw model 3500). The TLD reader showed variability by $\pm 12\%$ (coefficient of variation) over several years of readings. While some of the large changes in sensitivity were due to cleaning of the planchette, there is clearly substantial variation between days. Such variation must be accounted for to achieve reasonable accuracy in dose readings, meaning that $N_{D,w}$ must be determined for every reading session by irradiating and reading *standards* for that session. Other than that, the correction factors can be a function of the read-out procedure; energy dependence of TLD, for example, has been found to vary with maximum read-out temperature. (Tedgren et al, 2011).

For annealing, TLD is annealed for released all trapped electrons and store signal in the detector is removed. Despite of that, annealing pre and post irradiation also effect the glow curve and sensitivity of the detector. It is crucial to maintain the sensitivity of the detectors and follow a consistent annealing procedure.

The general consensus on the optimal annealing procedure for LiF,Mg,Ti is to anneal for 1 h at 400°C followed by 16–24 h at 80°C, although shorter annealing periods may suffice. The high-temperature component eliminates the previous dose information while the low-temperature component restores the original shape of the glow curve thus maintaining the sensitivity of the TLD. With careful annealing, the sensitivity of each TLD will change minimally, including both the average sensitivity of the TLDs and the relative sensitivity of each element ($k_{s,i}$). However, because sensitivity is highly dependent on the heating and cooling cycles, this is challenging to achieve. Therefore, all TLDs in a batch should be annealed together to ensure that their heating and cooling histories are all the same and therefore preserve their relative sensitivities (Kry et. al, 2020).

2.7 Comparison Dose-Area-Product (DAP) and Computed Tomographic Dose Index (CTDI) in dental CBCT.

Dose-Area-Product (DAP) and Computed Tomography Dose Index (CTDI) are frequently used for dose assessment. DAP is measured in mGy.cm² meanwhile CTDI in mGy. DAP is quantifying the total radiation output based on radiation in intensity and irradiated area. Then, CTDI is dose deposition within a standardized phantom slice. Both DAP and CTDI serves as valuable tools for quality assurance and dose comparison. CTDI is used to estimate the radiation dose at the lens during CBCT scans. Studies show that CBCT can reduce lens exposure compared to traditional CT, with a ratio of 1.1 for overall dose and 2.3 specifically at the lens (Shimada et al., 2017). DAP provides a broader perspective on radiation exposure, accounting for the area irradiated. It is particularly relevant in assessing cumulative exposure over multiple scans (Merce et al., 2018).

Some of studies using phantoms model have shown that there is weak to moderate correlation between DAP and eye lens dose based on CBCT protocol settings. Pauwels et al. (2014) reported that 45% reduction in lens dose could be achieved through protocol adjustment such as reducing the FOV and employing partial arc rotation (e.g. 180° instead of 360°). These findings in this study support the rationale protection of eye lens while the DAP and CTDI values reflect the dose trends, patient-specific anatomical and procedural factors heavily influencing the actual absorbed dose at eye lens.

CHAPTER 3

RESEARCH METHODOLOGY

This chapter outlines the research design and experimental methods employed to assess the absorbed dose to the eye lens during dental CBCT imaging. It details the materials and equipment used in the study, including the anthropomorphic head phantom, TLD-100 dosimeters, and the CBCT system. Additionally, the procedures for TLD sensitivity testing, calibration, and dose measurement across various CBCT acquisition protocols are described comprehensively.

3.1 Study Design

This study was designed as an experimental study using a head phantom to measure the absorbed dose to the eye lens. The primary objective was to evaluate and compare radiation dose levels across various CBCT acquisition protocols commonly used in clinical practice. By simulating realistic imaging conditions, the study aimed to assess dose variations attributable to differences in scanning parameters such as field of view (FOV), exposure settings, and rotation angles. The findings are intended to support dose optimisation strategies and enhance radiation safety, particularly concerning sensitive organs like the eye lens.

3.2 Study Location



Figure 3.2 This study was conducted at Institut Perubatan dan Pergigian Termaju Advanced

Medical and Dental Institute (IPPT)

This study was conducted at the Imaging Unit and the Physics Room, Oncology and Radiotherapy PPUSM at Advanced Medical and Dental Institute (AMDI), USM, Bertam, Penang.

3.3 Research Tools

3.3.1 ATOM Max Dental and Diagnostic Head Phantom Model 711-HN

A head phantom ATOM Max Dental and Diagnostic Head Phantom Model 711-HN is used a reference tool for diagnostic radiology of the head. It is specifically designed for monitoring, selection verification and training in various radiological procedures required fine anatomical defects. This phantom is used to evaluate and optimise scanning parameters in dental x-ray, panoramic, CT, and CBCT.



Figure 3.3.1 ATOM Max Dental and Diagnostic Head Phantom Model 711-HN (PEO Medical, 2015)

The phantom is made of tissue simulating hard epoxy resins, which is accurately mimic the x-ray attenuation properties of actual human tissues for both CT and Therapy energy ranges (50 keV - 25 MeV) (Sun Nuclear, n.d). The approximate dimensions of head phantom are 18 cm x 22.3 cm x 27 cm, meanwhile the weight is 6.4 kg (14 lbs). The stand of head phantom is included and adjustable in the x-y-z axes as well as allowing rotations about each of these exes. The weight of stand is 4 kg (9 lbs). The head is easily screws onto the stand and locks into place.